POLYVINYL-ALCOHOL (PVA)-BASED RF HUMIDITY SENSOR IN MICROWAVE FREQUENCY

Emran Md Amin[1, *], Nemai Karmakar[1], and Bjorn Winther-Jensen[2]

[1]Department of Electrical and Computer Systems Engineering, Bldg 72 Clayton Campus, Monash University, VIC 3800, Australia

[2]Department of Materials Engineering, Building 23 South Wing, Clayton Campus, Monash University, VIC 3800, Australia

Abstract—A highly sensitive, passive relative humidity (RH) sensor using polyvinyl-alcohol (PVA) dielectric film is presented. For the first time, PVA is investigated in microwave RF sensing devices for low cost, high resolution and accurate chipless RH sensor realization. Comparative study with traditional humidity sensing Kapton polymer is presented to validate superior performance of PVA film. Results are presented for two different passive high Q resonators to validate sensing performance in wide applications. Moreover, a new sensing parameter is described to investigate sensitivity measurement through resonance frequency and Q factor variation. The RH sensor has the potential to be integrated with mm and μm-wave high frequency passive RFID for ubiquitous sensing.

1. INTRODUCTION

Relative humidity (RH) is one of the most important physical parameters for assessment of air quality in controlled rooms, monitoring food conservation, detecting water damage in enclosed walls, buildings, and archives [1]. There is a demand for precise, consistent, robust, passive and low-cost sensor for RH measurement. Researchers are working towards a RH sensor having high sensitivity, wide dynamic range, stability, low hysteresis and ease of mass-production. In this regard, the investigation on humidity sensing layer materials for humidity sensor is one of the prime focuses of research [2]. For instance, humidity sensor based on ceramic sensing materials was reported in [3, 4]. These materials are oxide based sensing materials

including Al_2O_3, TiO_2 and SiO_2, independent of temperature, and sensitive to low humidity levels. In contrast, polymer-based humidity sensors have humidity sensitivity for wide moisture conditions. Most of the sensing polymers are either hydrophilic or hydrophobic, which implies that they show considerable structural reform in presence of water [5]. Hence these materials exhibit conductive or dielectric change with environmental humidity which can be quantified for RH monitoring.

Humidity sensors utilizing the change of electrical property of a material can be categorized in two types, resistive and capacitive sensors. Capacitive sensors have the features of ease of fabrication, low power requirement and linear response. Capacitive sensors utilize a hygroscopic dielectric layer whose dielectric constant changes with environmental RH [6]. Humidity sensors using polyvinyl-alcohol (PVA) as sensing dielectric was reported in [7, 8]. In [7], humidity sensor was fabricated with comb shaped electrodes coated with PVA. In [9] PVA coated SAW devices was reported to have significant humidity sensitivity. The RH sensitivity of PVA based SAW sensor was presented in regards of dynamic range, calibration curve, hysteresis and comparative analysis [8]. In [10] dielectric properties of PVA in aqueous solutions is reported upto 20 GHz frequency. However, the RF properties of PVA polymer has not yet been investigated in mm and μ-wave frequency range for passive RH sensing. Particularly, there is a huge potential of integrating sensing mechanism with passive chipless RFID technology which opens a new horizon of automated tracking and sensing applications [11–13]. The goal of this paper is to investigate RH sensing behavior of PVA polymer in Ultra high frequency (UHF) and Super high frequency (SHF) in line with the RF characterization presented in literatures. Moreover, RH sensitivity of PVA is compared with a commercially available dielectric hygroscopic polyamide Kapton [14]. Kapton has been widely used as a capacitive sensing layer for linear response, inexpensive and ease of availability [15]. Results presented in this paper demonstrate superior RH sensitivity of PVA over Kapton for both frequency bands. Also, RH sensitivity curve is determined to realize real time RH monitoring. In addition to resonant frequency shift, a novel parameter 'resonance slope' is introduced in this paper to determine accurate RH sensitivity. Undoubtedly, PVA shows great potential in realizing passive, low-cost, high-resolution RFID sensor in mm and μm wave frequency range.

2. THEORY OF HUMIDITY SENSING

A coplanar waveguide (CPW) line consists of a dielectric substrate with an infinite length center strip line on the top surface. The

strip line is separated by a narrow gap from two ground planes on either side. In this arrangement, the top plane of the CPW line is filled with air having permittivity ε_0. The size of (i) the center strip (S), (ii) the gap (W), (iii) the height (h_1), and (iv) the relative permittivity (ε_{r1}) of the substrate determines the effective dielectric constant and characteristics impedance of the line (Fig. 1). However, the transmission properties of a CPW line sandwiched between two dielectric substrates depend also on the height (h_2) and relative permittivity (ε_{r2}) of the top dielectric [16]. The characteristics impedance (Z_0) of a CPW line between two dielectrics is given by,

$$Z_0 = \frac{30\pi}{\sqrt{\varepsilon_{\mathit{eff}}}} \frac{K(k_0')}{K(k_0)} \tag{1}$$

Here, $\varepsilon_{\mathit{eff}}$ is the effective dielectric constant and $K(k_0)$ the modulus of complete elliptic integrals,

$$k_0 = \frac{S}{S + 2W} \tag{2}$$

$$k_0' = \sqrt{1 - k_0^2} \tag{3}$$

Also, the effective dielectric constant is given by,

$$\varepsilon_{\mathit{eff}} = 1 + q_1(\varepsilon_{r1} - 1) + q_2(\varepsilon_{r2} - 1) \tag{4}$$

Here, q_1 and q_2 are the partial filling factor depending on the structural parameters of a CPW line [17].

From (2)–(4), an imperative conclusion can be drawn about sensing mechanism. For a CPW line shown in Fig. 1, the characteristics impedance can be related with the top dielectric properties. Hence, a top dielectric with hydrophilic/hydrophobic nature can be used to incorporate relative humidity change to the CPW line parameters. This principle is used in our proposed microwave resonator to incorporate humidity sensing. As the top dielectric changes its relative permittivity (ε_{r2}) with humidity, the resonant condition varies
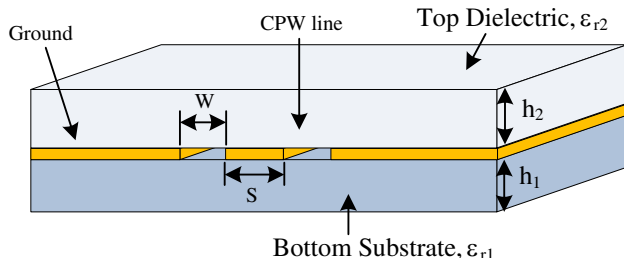
Figure 1. CPW line with top dielectric for sensing polymer.

accordingly. The variation of resonant frequency and Q factor variation at resonance can be calibrated against the humidity for monitoring real time environment conditions.

3. HUMIDITY SENSING POLYMERS

In this research, two moisture absorbing polymers have been investigated for passive humidity sensing. Table 1 summarizes their humidity sensing properties.

Table 1. Summary of humidity sensitivity parameter values for Kapton and PVA.

Humidity sensing Polymer	Formula	Effect of humidity change
Kapton	$C_{12}H_{12}N_2O$	• Kapton has been introduced in UHF RFID humidity sensors [14] • During moisture absorption, hydrolysis effect takes place which modifies the internal electrical polarization. • Kapton polyamide has a linear change with humidity according to the datasheet by Dupont. Kapton film has relative permittivity of 3.25 at 25% humidity and room temperature 23° C. At this temperature, Kapton's relative permittivity (ε_r) changes linearly with humidity (RH) given by, $\varepsilon_r = 3.05 + 0.008 \times RH$ • The dissipation factor changes from 0.0015 at 0% humidity to 0.0035 at 100%
PVA-Polyvinyl alcohol [18]	$[-CH_2CHOH-]_n$	• PVA is a hygroscopic polymer having an OH group • It creates H-H bonds in presence of water molecule which changes its dielectric and conductive properties. • PVA can be added with other electrolyte polymers/ Ions for higher sensitivity • It shows humidity sensitivity at a wide frequency range (0.2-20 GHz) • It shows low hysteresis characteristics in sensing ambient humidity.

4. DESIGN OF MICROWAVE RESONATOR

In this study, humidity sensitivity of Kapton polymer and PVA is investigated for two different frequency ranges. These are 950–1050 MHz (Ultra high frequency-UHF band) and 6–7 GHz (Super high frequency-SHF band). The aim is to compare the RF sensing

properties of the two polymer materials for various frequency bands. Detail description and design of the resonators is as follows.

4.1. Stepped Impedance Resonator (SIR)

Stepped impedance resonators (SIRs) are transmission line resonators utilizing quasi-TEM modes. SIRs have advantages over uniform impedance resonators (UIR) in their wide degree of freedom of design, compact size and ease of fabrication [19]. The basic structure of a three element half wave SIR is shown in Fig. 2(a).
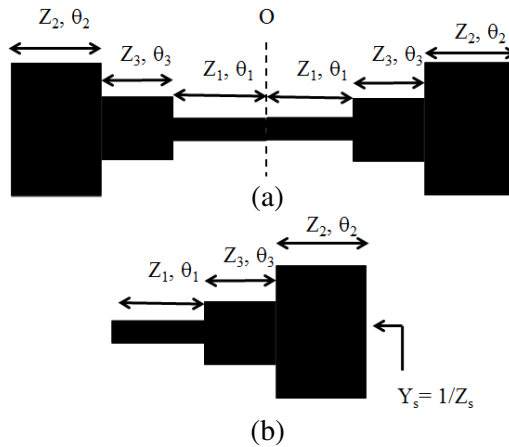
Figure 2. Layout of proposed (a) half wave tri-step SIR structure, (b) quarter wave SIR.

This structure is symmetric at the mid center 'O' and comprises of two cascaded quarter wave tri-step SIRs as shown in Fig. 2(b). The characteristic impedance of the three steps is Z_1, Z_2 and Z_3 having electrical length θ_1, θ_2 and θ_3. Thus, the overall electrical length of the half wave SIR is, $2\theta_T = 2(\theta_1+\theta_2+\theta_3)$. An open ended $\lambda/2$ type SIR resonates at a frequency corresponding to the total electrical length. At the resonant frequency the structure acts as a bandstop filter, attenuating most of the transmitted power. The overall admittance Y_s looking into the open end in Fig. 2(b) can be calculated from the equivalent impedance Z_s [20],

$$Z_s = \frac{j\left(Z_1 Z_2 \tan\theta_2 + Z_1 Z_3 \tan\theta_3 + Z_1^2 \tan\theta_1 - \frac{Z_1^2 Z_2}{Z_3} \tan\theta_1 \tan\theta_2 \tan\theta_3\right)}{\left(Z_1 - Z_2 \tan\theta_1 \tan\theta_2 - Z_3 \tan\theta_1 \tan\theta_3 - \frac{Z_1 Z_2}{Z_3} \tan\theta_2 \tan\theta_3\right)}$$

$$(5)$$

The resonance condition of tri-step SIR is $Y_s = 0$ which gives a relation between electrical length and step impedances discussed in [21]. A compact size SIR filter can be achieved by performing parametric study on (5) at resonance condition.

A CPW stepped impedance resonator (SIR) is designed in CST Microwave Studio operating at 1025 MHz. To create a SIR structure in a CPW line, the microstrip SIR structure is cut away from the continuous 50 ohm line. The simulation is performed on Taconic TLX-0 substrate having relative permittivity $\varepsilon_r = 2.45$ and $\tan \delta = 0.0019$ and substrate thickness, $h_1 = 0.5$ mm. The layout of the SIR filter is shown in Fig. 3.

Figure 4 shows the simulated magnitude of return loss (S_{11}) and insertion loss (S_{21}) vs frequency. The filter operates as a bandstop
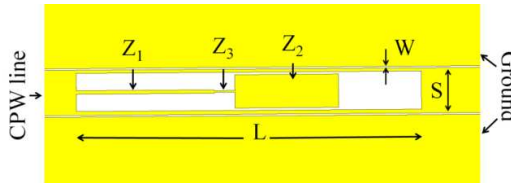
Figure 3. Layout of the tri section SIR at 1025 MHz. The length and width of Z_1, Z_2 and Z_3 sections are 15 mm and 4.8 mm; 22.4 mm and 0.5 mm; 3.0 mm and 0.25 mm. Total Length, $L = 50$ mm; $W = 0.25$ mm; $S = 0.65$ mm. The simulation is performed on Taconic TLX0 substrate having relative permittivity $\varepsilon_r = 2.45$ and $\tan \delta = 0.0019$ and substrate thickness, $h = 0.5$ mm. The CPW line is matched to 50 Ohms.
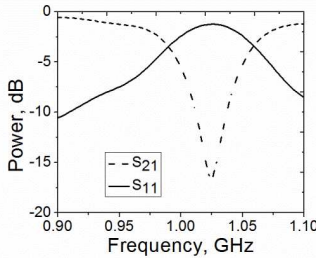
Figure 4. Simulated reflection loss (S_{11}) and insertion loss (S_{21}) vs frequency of SIR resonator.
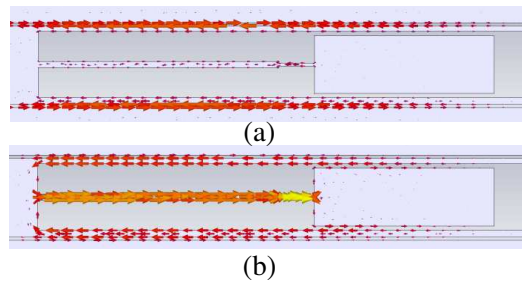
Figure 5. Surface current distribution of the SIR structure at (a) 1.5 GHz (outside resonant condition) and (b) 1.025 GHz (resonant condition).

filter at 1025 MHz having about 20 dB attenuation. The resonance characteristics are explained using the surface current distribution in Fig. 5. The surface current density is maximum along the edge of CPW line at 1.5 GHz frequency (Fig. 5(a)). At this frequency, charge distribution along the SIR structure is negligible as it is outside the resonance band. However, at the resonant frequency (1025 MHz), there is an intense current density along the SIR structure which results in signal attenuation at the receiving end (Fig. 5(b)).

4.2. Electric Field Coupled Inductor Capacitor (ELC) Resonator

An ELC resonator proposed in [22] is designed to incorporate humidity sensing at SHF frequency. An ELC resonator couples strongly to a polarized incident E field and marginally to a uniform H field. The layout of an ELC resonator is shown in Fig. 6. As, a plane wave illuminates the resonator, the middle capacitor like structure couples to the E field and is connected to two parallel loops, which provide the inductance. Thus, the structure resonates at a frequency determined by its equivalent L and C components. Here, the capacitance generated between two split gaps of the ELC resonator has a major influence in
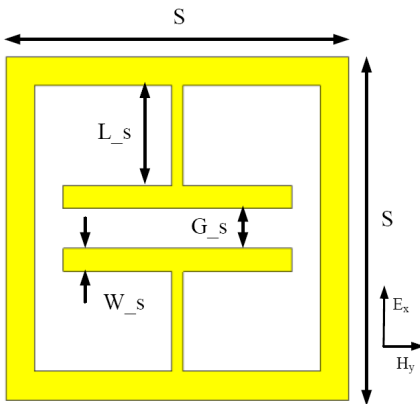
Figure 6. Layout of ELC resonator. The dimensions are S = 6 mm; L_s = 1.75 mm; G_s = 0.7 mm; W_s = 0.4 mm. Substrate Taconic TLX_0; height, h = 0.5 mm; ε_r = 2.45; $\tan \delta$ = 0.0019.
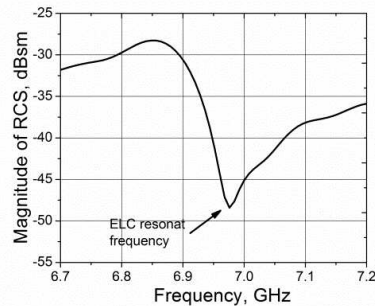
Figure 7. Simulated RCS magnitude vs frequency for the ELC resonator at 6.96 GHz.

the structures resonance frequency.

For our tag sensor, an ELC resonator is designed that resonates at 6.96 GHz. The parametric values of the ELC resonator are shown in Fig. 6. Also, Fig. 7 shows the simulated RCS magnitude of the backscattered signal when the structure is interrogated using a vertically polarized plane wave.

As stated before, the ELC resonator has high E field concentration between the capacitor plates at resonance. Fig. 8(a) shows the E field concentration at a frequency outside resonance. Here the E field is negligible compared to Fig. 8(b) where, a prominent electric field is observed at resonant frequency.

(a)   (b)
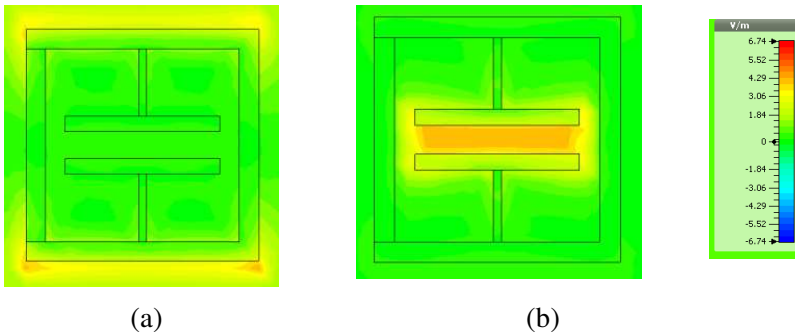
Figure 8. (a) Simulated E-field concentration at a frequency outside resonance for ELC resonator. (b) E-field concentration at resonance.

5. EXPERIMENT FOR HUMIDITY SENSING

5.1. Experimental Set-up

To validate humidity sensing of the two polymers, an experiment is performed using Miller Nelson Temperature and Humidity controller [26]. A photo of our experimental setup is shown in Fig. 9. Here, the humidity controller is connected to an esky chamber through a water flow sensor. The esky has an air tight lid so that its temperature and humidity can be controlled. Our sensor and a DIGITECH QP-6013 data logger is placed inside the chamber. The data logger reads and stores the temperature and humidity inside the chamber at regular time interval. A vector network analyzer (VNA) is used for frequency response measurement. By changing the set temperature and humidity of Miller nelson controller we measured the response of the resonators for different environment conditions. In
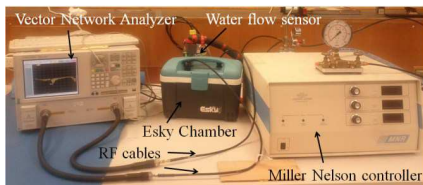
Figure 9. Experimental set-up for humidity controller. The sensor is placed inside the enclosed Esky chamber for measuring transmission coefficient.
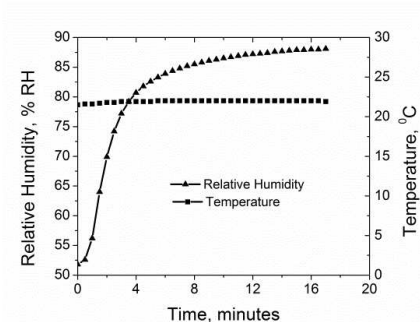
Figure 10. Plot of relative humidity and temperature against time measured inside the chamber using data logger during experiment for humidity sensor.

Fig. 10, temperature and humidity records captured from the data logger during the experiment is plotted. It shows an almost constant temperature of about $22.5°C$ throughout the total time span. However, the RH changed from 50% to 90% inside the chamber.

The experimental setup is used for comparing humidity sensitivity of Kapton and PVA at two different frequency bands as described in the following sections.

5.2. Humidity Sensing with SIR Resonator at 950–1050 MHz

According to the design, SIR structure is fabricated on Taconic TLX-0 substrate. Copper is etched out to create the microwave structure. A photograph of the fabricated SIR filter operating at 1025 MHz is shown in Fig. 11(a). The frequency response of fabricated SIR filter is measured using a two port VNA (Fig. 12). The measured insertion loss (S_{21}) and reflection loss (S_{11}) corresponds to the simulated results shown in Fig. 4.

To incorporate humidity sensing using Kapton, a Kapton HN [17] adhesive tape of 0.1 mm thickness is attached to the top surface of CPW SIR resonator (Fig. 11(b)). The SIR filter with Kapton tape operates as a humidity sensor according to the theory discussed before. The resonator is then connected to the two ports of the VNA inside the esky chamber and its S_{21} is measured for various humidity conditions (Fig. 13(a)). Measured results show a steady shift of the resonant frequency with RH. The total frequency shift is 25 MHz for RH change of (50%–90%).

(a)

(b)
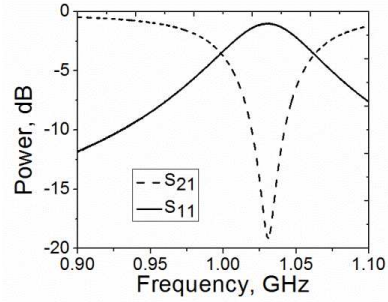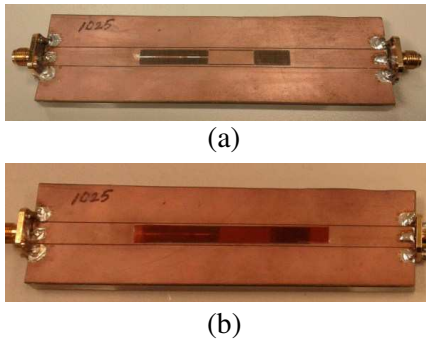
Figure 11. Photo of fabricated SIR structure for humidity sensing (a) without Kapton coating, (b) with Kapton coating.

Figure 12. Magnitude of measured reflection loss (S_{11}) and insertion loss (S_{21}) vs frequency.

(a)

(b)
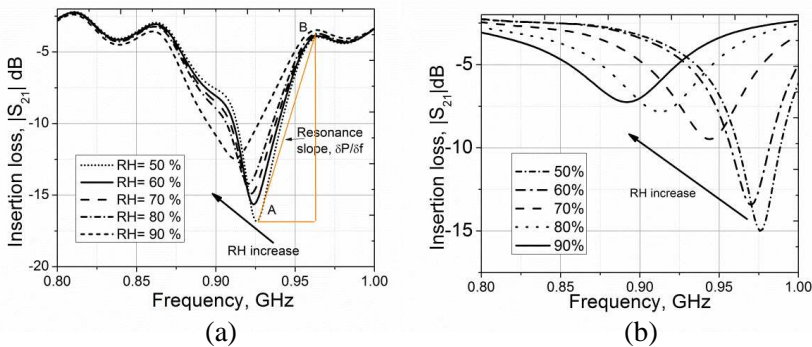
Figure 13. (a) Magnitude of measured insertion loss (S_{21}) vs frequency for different humidity conditions with Kapton. (b) Magnitude of measured insertion loss (S_{21}) vs frequency for different humidity conditions with PVA.

The increased moisture in air increases permittivity of Kapton film. This enhances the total capacitance of the SIR filter on CPW line which is observed as resonance shift. Also, the Q factor of the resonator is changed at high humidity conditions. This is due to the imaginary permittivity, ε_r' variation with RH. To quantify the effect of Q factor variation, a parameter 'resonance slope' is defined as, $\delta P/\delta f$. Here, δP is the power difference at resonant frequency (A) and at the immediate maximum point (B) (refer to Fig. 13(a)). Also, δf

is the frequency deviation between point A and B. Hence, this slope $\delta P/\delta f$ gives an indication of Q factor variation which decreases with RH increase. Detail on 'Resonance slope' parameter is discussed in Section 6.

To incorporate humidity sensing using PVA polymer, a thin layer of PVA 31-50000 is coated on top of the SIR resonator. The PVA polymer is acquired from Sigma Aldritch and it is dissolved in a solution of H_2O/Ethanol 3/1 for about 3 hours through magnetic stirring. Afterwards it became completely soluble and transparent. Then, it is carefully poured on top of the SIR structure using a fine droplet. It is then dried to have a 0.1 mm coating of PVA on top of SIR structure. Fig. 13(b) shows the measured S_{21} in dB vs frequency for SIR resonator. Compared to Kapton, PVA shows strong sensitivity to environment moisture and the total frequency shift measured is 95 MHz for RH change of (50%–90%). Also, the resonance slope variation is prominent in case of PVA compared to Kapton for equivalent change in RH.

5.3. Humidity Sensing with ELC Resonator at 6.0–7.0 GHz

An ELC resonator is fabricated on Taconic TLX-0 substrate having the dimensions shown in Fig. 5. Fig. 14 shows the photo of fabricated ELC. The structure is one sided RCS scatterer. Two horn antennas operating from 5.5 GHz to 12 GHz (less than -10 dB band) is used to measure the transmission coefficient (S_{21}) of our ELC resonator. Fig. 15 plots measured S_{21} vs frequency. It shows a resonant frequency at 6.96 GHz.

In this experiment, relative humidity inside the esky chamber

Figure 14. Photo of fabricated ELC resonator with PVA coating.
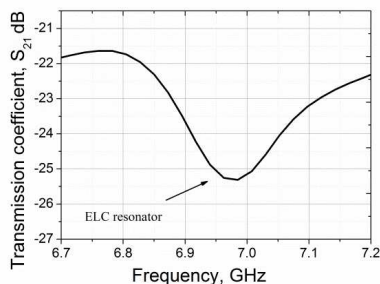
Figure 15. Magnitude of measured transmission coefficient (S_{21}) vs frequency for ELC resonator.
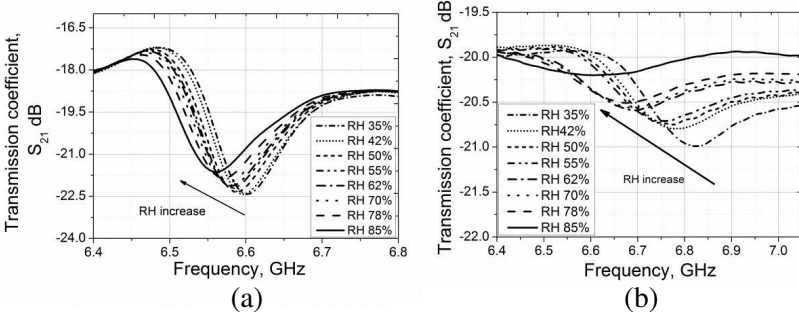
Figure 16. (a) Magnitude of Measured transmission coefficient (S_{21}) vs frequency for different humidity conditions with Kapton. (b) Magnitude of Measured transmission coefficient (S_{21}) vs frequency for different relative humidity conditions with PVA.

is varied from 35% to 85%. Fig. 16(a) and Fig. 16(b) show the transmission coefficient of ELC resonator with Kapton and PVA as superstrate respectively. Here, the maximum frequency shift for PVA and Kapton is measured as 270 MHz and 67 MHz. The sensitivity curve for the two polymers is explained in the next section.

6. SENSITIVITY CURVE

In this study, the sensitivity curve for humidity sensing polymers is analyzed taking two parameters into account: (1) Resonant frequency (f_r) and (2) Resonance slope parameter $(\delta P/\delta f)$. Sensitivity curve for f_r plots the measured resonant frequency at different RH. Whereas, sensitivity curve for $(\delta P/\delta f)$ plots the normalized resonance slope at different RH. Here, the slope at minimum RH is taken as reference for normalizing.

Sensitivity curves of these two parameters for Kapton and PVA at frequency (950–1050 MHz) is shown in Fig. 17(a) and Fig. 17(b). Also, Figs. 18(a)–(b) show the sensitivity curve for frequency range (6–7 GHz). To calculate sensitivity for 1% RH change, the following formula is used,

$$S_\gamma = \frac{|\Delta\gamma|}{|\Delta RH|} = \frac{|\gamma(RH_{high} - RH_{low})|}{|RH_{high} - RH_{low}|} \quad (6)$$

Here, γ donates to resonant frequency or normalized resonance slope parameter. Table 2 summarizes the sensitivity S_{fr} and $S_{\delta P/\delta f}$ for the two polymers with different resonators. The sensitivity values
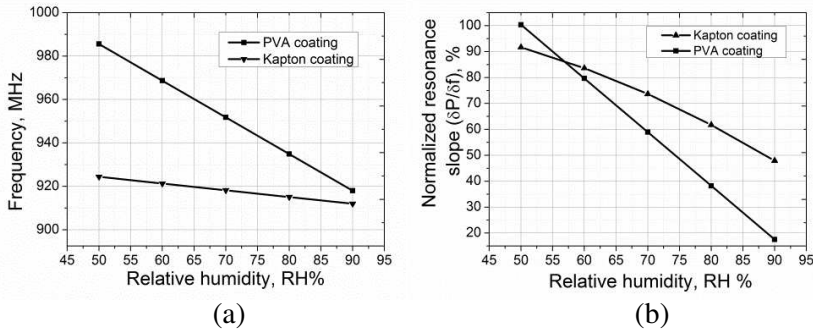
Figure 17. (a) Measured sensitivity curve of the SIR resonator for resonant frequency (f_r) vs relative humidity (RH). (b) Measured sensitivity curve of the SIR resonator for resonance slope parameter ($\delta P/\delta f$) vs relative humidity (RH).
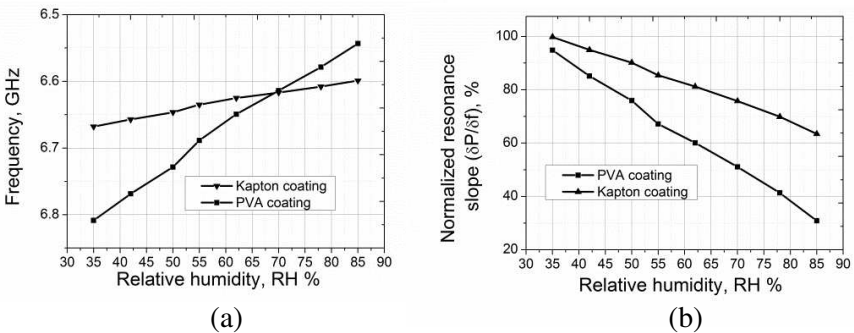
Figure 18. (a) Measured sensitivity curve of the ELC resonator for resonant frequency (f_r) vs relative humidity (RH). (b) Measured sensitivity curve of the ELC resonator for resonance slope parameter ($\delta P/\delta f$) vs relative humidity (RH).

calculated in Table 2 essentially is the slope of the curves shown in Fig. 17 and Fig. 18.

6.1. Kapton HN Polyamide

Kapton polyamide is a hydrophobic organic material and operates as a capacitive humidity sensor. It has linear dielectric response while absorbs water as the weight is proportional to RH. The structural

Table 2. Summary of humidity sensitivity parameter values for Kapton and PVA.

Humidity sensitive polymers	SIR resonator		ELC resonator	
	S_{fr} (MHz/RH)	$S_{\delta P/\delta f}$ (%/RH)	S_{fr} (MHz/RH)	$S_{\delta P/\delta f}$ (%/RH)
Kapton	0.63	1.02	1.68	0.7
PVA	2.38	2.1	6.75	1.4

formula is shown in Fig. 19 which absorbs water between the free space of adjacent polymeric molecules [15]. A linear dielectric behavior of Kapton film with RH is reported. For 100% RH variation, its dielectric constant changes about 25%. The enhanced dielectric constant induces capacitance which is reflected as frequency shift in S_{21} response. The frequency variation is 0.63 MHz for SIR resonator and 1.68 MHz for ELC resonator for 1% RH change. On the other hand, Kapton exhibits a linear increase of dissipation factor with humidity [14]. This implies, at higher humidity, Kapton has more dielectric loss which degrades the Q factor of the resonators. This effect is calibrated by determining normalized resonance slope parameter ($\delta P/\delta f$) at various RH as shown in Fig. 17(b) and Fig. 18(b). For both resonators, the slope parameter value decreased about 50% at maximum humidity compared to its initial value. Also, the sensitivity of normalized $\delta P/\delta f$ for 1% RH change is 1.02% and 0.7% for SIR and ELC resonator respectively. This implies at high frequency, the Q factor variation is less prominent for Kapton.

6.2. PVA Polymer

PVA is hydrophilic in nature and thus, can be used as a polyelectrolyte based resistive sensor. A detail chemical formula of PVA polymer chain is shown in Fig. 20. In [10, 23] the microwave frequency characteristics of PVA in aqueous solution was reported. In these studies, the dielectric behavior of water is investigated as the temperature and PVA concentration is changed. It shows that as the PVA concentration in water increases, the real part of permittivity ε'_r decreases at any frequency (0.2–20 GHz). At frequency range (6–7 GHz), PVA has a dielectric constant change of 75% for only 20% increase in water content in a water-PVA solution [23]. The sensitivity curve for resonant frequency Fig. 17(a) and Fig. 18(a) corresponds to the increased permittivity of PVA sensor with RH. Compared to Kapton, PVA sensor exhibits higher resonant frequency shift for 1% RH change. Also, at high frequency (6–7 GHz), it has the maximum value of
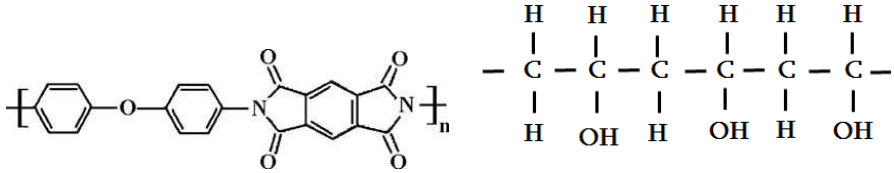
Figure 19. Chemical formula of Kapton polyimide [18].

Figure 20. Chemical formula of PVA [27].

6.75 MHz/%RH for ELC resonator.

In addition, the normalized resonance slope parameter $(\delta P / \delta f)$ of PVA sensor varies significantly for both resonators (Fig. 17(b) and Fig. 18(b)). From the measured results, the slope parameter value decreases about 20% of its initial value at maximum humidity. Also, the sensitivity of normalized slope parameter for PVA is about 2 times of Kapton for both SIR and ELC resonators. This verifies for equivalent RH change, and PVA exhibits greater dielectric loss and essentially higher sensing resolution. Finally, at high frequency, the Q factor variation is less prominent for PVA similar to Kapton (column 2 and 4 of Table 2). The change of Q factor is due to the imaginary relative permittivity (ϵ_r'') variation with water absorption. In [10] a study on dielectric dispersion of PVA in aqua solution was presented. It was reported that, in PVA aqua solution, the ϵ_r changes due to the breaking and reforming of hydrogen bonds of water molecules with '-OH' groups present in PVA chain. This attributes high dielectric loss (ϵ_r'') as PVA absorbs water.

The variation of resonance slope parameter gives an indication of Q factor change which essentially can be calibrated as sensing parameter. Along with resonance frequency, this new parameter can carry additional information about RH and increase sensing accuracy and reliability. From Table 2, it is evident that for both resonators, PVA shows excellent humidity sensitivity over Kapton polyamide. The measured humidity sensitivity of PVA at microwave frequency indicates its potential for integrating in passive RF sensors to monitor environment humidity. Also, the results presented here illustrates superior sensitivity of PVA polymer compared to previous reported works on humidity sensor [8].

6.3. Hysteresis Analysis

Hysteresis analysis is performed to study the repeatability of humidity sensors. For our sensors, the hysteresis depends primarily on the

polymer material properties. In case of Kapton film, hydrolysis effect alters its internal electrical polarization which effectively manifests permittivity change. In [24], hysteresis analysis for Kapton film is thoroughly investigated. It shows linear repeatability for Kapton film. However, the time for stability is high. In contrast, PVA film has short term repeatability as reported in [7, 8]. This makes PVA film suitable for reproducible real world applications.

An experiment is performed to investigate hysteresis effect of ELC resonator coated with PVA film. In the esky chamber, RH is increased from 35% to 85% then decreased back to 35%. Results are measured in 1 hour increments to ensure full absorption of water. Fig. 21 shows the resonant frequency vs RH during water absorption and desorption. At high humidity conditions (80–90% RH) there is a trivial hysteresis observed. However, at lower humidity, the two curves almost coincide.
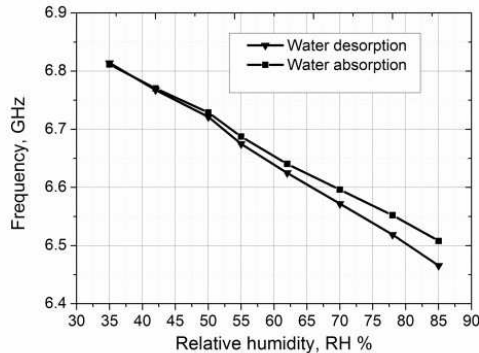
Figure 21. Resonant frequency vs RH for PVA film coated ELC resonator during water absorption and desorption.

7. CONCLUSION

This paper presents a very low cost passive microwave frequency relative humidity sensor for wireless monitoring of perishable items. The novelty of our contribution is an investigation of RF sensing property of hygroscopic PVA film and Kapton polyamide. To the best of our knowledge, PVA has not been used in mm- and μ-wave devices for passive humidity sensing. Results confirm that PVA has superior RH sensitivity over conventional Kapton polyamide across a wide frequency range. Moreover, in microwave frequency, both the resonant frequency and Q factor variation become prominent in passive resonator circuits. This adds a new dimension in quantifying

sensing parameters as demonstrated in the measured results. Proper calibration curve has been determined to realize a real time RH sensor. This research will open up a new direction in microwave frequency passive RFID and sensing applications.

REFERENCES

1. Traversa, E., "Ceramic sensors for humidity detection: The state-of-the-art and future developments," *Sensors and Actuators B: Chemical*, Vol. 23, 135–156, 1995.

2. Sakai, Y., et al., "Humidity sensors based on polymer thin films," *Sensors and Actuators B: Chemical*, Vol. 35, 85–90, 1996.

3. Ansbacher, F. and A. C. Jason, "Effects of water vapour on the electrical properties of anodized aluminium," *Nature*, Vol. 171, 177–178, 1953.

4. Chen, Z., et al., "Humidity sensors with reactively evaporated Al_2O_3 films as porous dielectrics," *Sensors and Actuators B: Chemical*, Vol. 2, 167–171, 1990.

5. Rittersma, Z. M., et al., "A novel surface-micromachined capacitive porous silicon humidity sensor," *Sensors and Actuators B: Chemical*, Vol. 68, 210–217, 2000.

6. Harpster, T. J., et al., "A passive wireless integrated humidity sensor," *Sensors and Actuators A: Physical*, Vol. 95, 100–107, 2002.

7. Yang, M.-R. and K.-S. Chen, "Humidity sensors using polyvinyl alcohol mixed with electrolytes," *Sensors and Actuators B: Chemical*, Vol. 49, 240–247, 1998.

8. Penza, M. and G. Cassano, "Relative humidity sensing by PVA-coated dual resonator SAW oscillator," *Sensors and Actuators B: Chemical*, Vol. 68, 300–306, 2000.

9. Chen, Y. T. and H. L. Kao, "Humidity sensors made on polyvinyl-alcohol film coated saw devices," *Electronics Letters*, Vol. 42, 948–949, 2006.

10. Sengwa, R. J. and K. Kaur, "Dielectric dispersion studies of poly (vinyl alcohol) in aqueous solutions," *Polymer International*, Vol. 49, 1314–1320, 2000.

11. Amin, E. M. and N. C. Karmakar, "Development of a low cost printable humidity sensor for chipless RFID technology," *2012 IEEE International Conference on RFID-technologies and Applications (RFID-TA)*, 165–170, 2012.

12. Amin, E. M., et al., "Towards an intelligent EM barcode," *2012 7th International Conference on Electrical & Computer Engineering (ICECE)*, 826–829, 2012.

13. Girbau, D., et al., "Passive wireless temperature sensor based on time-coded UWB chipless RFID tags," *IEEE Transactions on Microwave Theory and Techniques*, Vol. 60, 3623–3632, 2012.

14. Virtanen, J., et al., "Inkjet-printed humidity sensor for passive UHF RFID systems," *IEEE Transactions on Instrumentation and Measurement*, Vol. 60, 2768–2777, 2011.

15. Chen, Z. and C. Lu, "Humidity sensors: A review of materials and mechanisms," *Sensor Letters*, Vol. 3, 2005.

16. Simons, R. N., *Coplanar Waveguide Circuits, Components, and Systems*, Wiley, 2001.

17. Gevorgian, S., et al., "CAD models for shielded multilayered CPW," *IEEE Transactions on Microwave Theory and Techniques*, Vol. 43, 772–779, 1995.

18. Ogura, K., et al., "The humidity dependence of the electrical conductivity of a solublepolyaniline-poly (vinyl alcohol) composite film," *Journal of Materials Chemistry*, Vol. 7, 2363–2366, 1997.

19. Sagawa, M., et al., "Geometrical structures and fundamental characteristics of microwave stepped-impedance resonators," *IEEE Transactions on Microwave Theory and Techniques*, Vol. 45, 1078–1085, 1997.

20. Zhang, H. and K. J. Chen, "A tri-section stepped-impedance resonator for cross-coupled bandpass filters," *IEEE Microwave and Wireless Components Letters*, Vol. 15, 401–403, 2005.

21. Zhang, H. and K. J. Chen, "Miniaturized coplanar waveguide bandpass filters using multisection stepped-impedance resonators," *IEEE Transactions on Microwave Theory and Techniques*, Vol. 54, 1090–1095, 2006.

22. Schurig, D., et al., "Electric-field-coupled resonators for negative permittivity metamaterials," *Applied Physics Letters*, Vol. 88, 041109, 2006.

23. Yeow, Y. K., K. Khalid, and M. Z. A. Rahman, "Improved dielectric model for polyvinyl alcohol-water hydrogel at microwave frequencies," *American Journal of Applied Sciences*, 2010.

24. Ralston, A. R. K., et al., "A model for the relative environmental stability of a series of polyimide capacitance humidity sensors," *The 8th International Conference on Solid-State Sensors and Actuators, 1995 and Eurosensors IX, Transducers'95*, 821–824, 1995.